Organic & Biomolecular Chemistry

Cite this: *Org. Biomol. Chem.*, 2011, **9**, 3217

www.rsc.org/obc

PAPER

An *ab initio* and DFT study of radical addition reactions of imidoyl and thioyl radicals to methanimine†‡

Sara H. Kyne,[a,b,c,d] Carl H. Schiesser[a,b,c] and Hiroshi Matsubara*[c,e]

Received 20th January 2011, Accepted 16th February 2011
DOI: 10.1039/c1ob05105a

Ab initio and DFT calculations reveal that both imidoyl and thioyl radicals add to the nitrogen end of methanimine through simultaneous SOMO-π^*_{imine}, SOMO-π_{imine}, SOMO-LP_N and $\pi^*_{radical}$-LP_N interactions between the radical and the imine. At the CCSD(T)/cc-pVDZ//BHandHLYP/cc-pVTZ level of theory, barriers of 13.8 and 26.1 kJ mol^{-1} are calculated for the attack of the methylimidoyl radical at the carbon- and nitrogen- end of methanimine, respectively, indicating that the imidoyl radial has a preference for addition to the nitrogen end of imine. On the other hand, barriers of 25.1 and 13.4 kJ mol^{-1} are calculated at the same level of theory for the addition reaction of the methanethioyl radical at the carbon- and nitrogen- end of methanimine, respectively. Natural bond orbital (NBO) analysis at the BHandHLYP/6-311G** level of theory reveals that SOMO-π^*_{imine}, SOMO-π_{imine}, SOMO-LP_N and $\pi^*_{radical}$-LP_N interactions are worth 111, 89, 115 and 17 kJ mol^{-1}, respectively, in the transition state (**4**) for the reaction of methylimidoyl radical at the nitrogen end of methanimine; similar interactions are observed for the chemistry involving all the radicals studied here. These multi-component interactions are responsible for the unusual motion vectors associated with the transition states involved in these reactions.

Introduction

Acyl radicals (O═C$^{\bullet}$–R) are convenient intermediates that can lead to the preparation of cyclic ketones, esters and amides, and are often generated from seleno- or telluro-esters.[1,2] In addition, Ryu and co-workers developed carbonylation methodology for the generation of acyl radicals and showed that various ring-systems could be constructed quickly and efficiently.[3] During this work it was noted that acyl radicals are N-philic, that is, they generally prefer attack at the nitrogen end of imine C═N double bond. Computational investigations[4–6] concluded that this phenomena was the result of simultaneous SOMO → π^*_{imine} and LP_N (lone pair of nitrogen of the imine) → $\pi^*_{C=O}$ interactions between the two reacting units (Scheme 1).

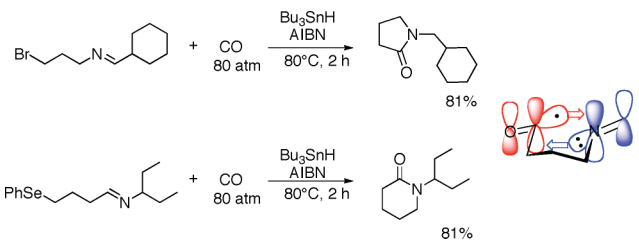

Scheme 1

Imidoyl radicals (R–N═C$^{\bullet}$–R′) and thioyl radicals (S═C$^{\bullet}$–R) have pseudo-isoelectronic structures compared with acyl radicals. Imidoyl radicals have been used as important intermediates in organic synthesis,[7,8] some examples of their synthetic utility are shown in Scheme 2.[9–11] Many studies on spectroscopy, kinetics and structures of imidoyl radicals have also been reported.[12] Guerra has used *ab initio* calculations to investigate the geometries of silyl-substituted imidoyl radicals,[13] however apart from this example, theoretical studies of imidoyl radicals are rare.[14] On the other hand, sulfur containing radicals related to acyl radicals have two types of combinations of sulfur and oxygen atoms, namely, alkyl-thio-acyl radicals (O═C$^{\bullet}$–SR) and thioyl radicals (S═C$^{\bullet}$–R). The former radicals are used in organic synthesis[15] and we have previously carried out a theoretical study involving this species.[16] The latter

[a]*School of Chemistry, The University of Melbourne, Victoria, 3010, Australia*
[b]*Bio21 Molecular Science and Biotechnology Institute, The University of Melbourne, Victoria, 3010, Australia*
[c]*ARC Centre of Excellence for Free Radical Chemistry and Biotechnology, Australia*
[d]*Current address: WestCHEM Department of Pure and Applied Chemistry, University of Strathclyde, Glasgow, UK, G1 1XL*
[e]*Department of Chemistry, Graduate School of Sciences, Osaka Prefecture University, Sakai, Osaka, 599-8531, Japan. E-mail: matsu@c.s.osakafu-u.ac.jp; Fax: +81 72 254 9163; Tel: +81 254 9698*

† This paper is dedicated to Professor Athel Beckwith.

‡ Electronic supplementary information (ESI) available: Optimized geometries (Gaussian archives entries) of all ground and transition states involved in this study at all levels of theory used here. A full list of energy barriers $\Delta E_1^{\ddagger}$ – $\Delta E_4^{\ddagger}$ for reactions involving N-methylmethylimidoyl radical ($\mathbf{1}_{Me}$). Optimized structures of transition states **5** and **6** involved in the addition of $\mathbf{1}_{Me}$. BHandHLYP/6-311G** calculated Kohn–Sham orbitals involved in transition states **5** and **6**. GaussView generated animations of the transition state vectors in **3**–**8** as Audio Video Interleave (AVI) files. See DOI: 10.1039/c1ob05105a

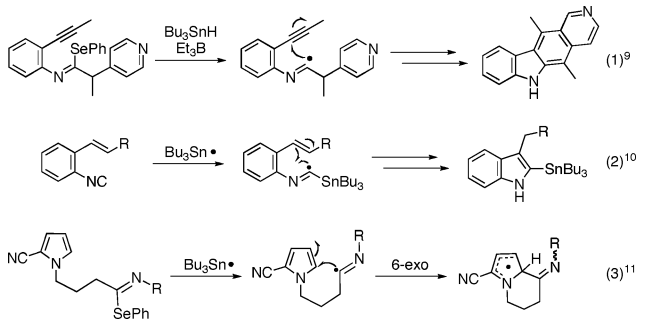

Scheme 2

radicals can only be detected by EPR,[17] and to our knowledge there have been no applications[18] of the radicals to organic synthesis as yet. Nevertheless, these radicals represent fascinating higher homologues of acyl radicals.

As part of our continuing interest in acyl radicals and related radical chemistry, we chose to explore intermolecular radical addition reactions of methylimidoyl (HN═C•–CH_3, $\mathbf{1_H}$), N-methylmethylimidoyl (H_3C–N═C•–CH_3, $\mathbf{1_{Me}}$) and methanethioyl (S═C•–CH_3, **2**) radicals to methanimine (HN═CH_2) through the use of *ab initio* and DFT calculations to gain insight into the characteristics of these reactions.

Methods

Ab initio and DFT calculations were carried out using the Gaussian 03 and 09 programs.[19] Geometry optimizations were performed using standard gradient techniques at the BHandHLYP level of theory using restricted (RBHandHLYP) and unrestricted (UBHandHLYP) methods for closed- and open-shell systems, respectively. In every case, standard basis sets were used. All ground and transition states were verified by vibrational frequency analysis. Further single-point QCISD, CCSD(T) and G3(MP2)-RAD[20] calculations were performed on each of the BHandHLYP/cc-pVTZ optimized structures. Scaling factors were not applied to the G3(MP2)-RAD calculations. When correlated methods were used, calculations were carried out using the frozen core approximation. Values of $<s^2>$ never exceeded 0.82 before annihilation of quartet contamination. Where appropriate, zero-point vibrational energy (ZPE) corrections without scaling have been applied. Natural Bond Orbital (NBO) analyses[21,22] were performed within the Gaussian 03 program.

Optimized geometries and energies for all transition and ground structures in this study (Gaussian Archive entries) are available in the ESI.‡

Results and discussion

Reaction of the methylimidoyl radical with methanimine

We began this investigation by examining the reaction of the methylimidoyl radical ($\mathbf{1_H}$) with methanimine, as representative examples of the key reaction components. As previous benchmarking studies have established that BHandHLYP is a reliable method for the study of acyl and related radical chemistry,[4–6] we chose to primarily use this method in the current investigation. Inspection of the $C_3H_7N_2$ potential energy surface located structures **3** and **4** as the lowest transition states for the reaction of the imidoyl radical at the carbon and nitrogen ends of the C═N bond in methanimine, respectively (Scheme 3). Transition states **3** and **4** are displayed in Fig. 1, along with important geometric features. Motion arrows associated with the transition state vector in each case are included and give insight into the attack trajectory of the imidoyl radical during addition to the imine.§ In particular, transition state **4** shows similar rocking motion ($\nu = 439$i cm^{-1}, BHandHLYP/6-311G**)¶ to its acetyl counterpart.[5] The transition state separations are observed to be larger for attack at the carbon end of the imine bond, with transition state **3** predicted to have separations between 2.21–2.24 Å, compared to transition state **4** with separations of 2.09–2.11 Å. While the separations in transition state **3** are predicted to be very close to the analogous transition states involving the acetyl radical, the separations in transition state **4** are elongated by approximately 0.15 Å. In addition, angles (θ) located around the carbonyl bond are predicted to be very similar for attack at the carbon to those for attack at the nitrogen. For example, at the BHandHLYP/cc-pVTZ level of theory, the angles for transition states **3** and **4** are calculated to be 113.0° and 112.8°, respectively. The calculated angles in transition state **3** are approximately 5° smaller than the angles for analogous transition states involving the acetyl radical while the angles in transition state **4** are larger by about 3° than those for the acetyl radical.

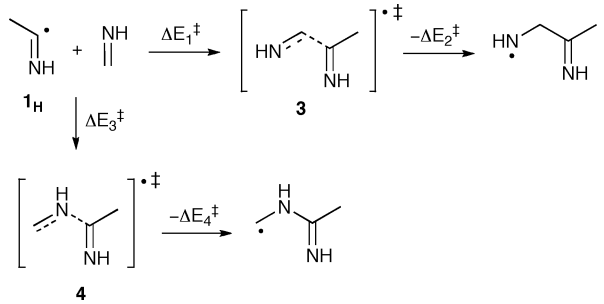

Scheme 3

Activation energy data (Scheme 3, $\Delta E_1^{\ddagger} - \Delta E_4^{\ddagger}$) calculated at various levels of theory are listed in Table 1. At all the levels of theory employed the reactions are predicted to be highly exothermic with calculated energy barriers ($\Delta E_2^{\ddagger}$ and $\Delta E_4^{\ddagger}$) for the reverse reactions (Scheme 3) always much larger than those ($\Delta E_1^{\ddagger}$ and $\Delta E_3^{\ddagger}$) for the forward process. Inspection of Table 1 reveals that the energy barriers for the forward reaction associated with transition states **3** and **4** are calculated to be 12.5 and 27.3 kJ mol^{-1}, respectively at the BHandHLYP/6-311G** level of theory. Inclusion of zero-point vibration energy correction (ZPE) serves to increase these barriers by about 5 kJ mol^{-1} while improvement of basis set quality and levels of correlation have little effect on these barriers. At the CCSD(T)/cc-pVDZ//BHandHLYP/cc-pVTZ level of theory, $\Delta E_1^{\ddagger}$ and $\Delta E_3^{\ddagger}$ are predicted to be 13.8 and 26.1 kJ mol^{-1}, respectively, while values of 14.0 and 27.6 kJ mol^{-1} are

§ Animations of the transition state imaginary frequencies are conveniently visualized using the GaussView software that complements Gaussian 03.[19] BHandHLYP/6-311G** generated animations of the transition state vectors in **3–8** are available in the ESI‡ as Audio Video Interleave (AVI) files.

¶ When the transition state vectors are animated using software such as GaussView.

Table 1 Calculated energy barriers[a] for the forward ($\Delta E_1^{\ddagger}$, $\Delta E_3^{\ddagger}$) and reverse ($\Delta E_2^{\ddagger}$, $\Delta E_4^{\ddagger}$) reactions of methylimidoyl radical with methanimine and imaginary frequencies (ν)[b] of transition states **3** and **4** (Scheme 3)

	3					**4**				
Method	$\Delta E_1^{\ddagger}$	$\Delta E_1^{\ddagger}$ + ZPE	$\Delta E_2^{\ddagger}$	$\Delta E_2^{\ddagger}$ + ZPE	ν	$\Delta E_3^{\ddagger}$	$\Delta E_3^{\ddagger}$ + ZPE	$\Delta E_4^{\ddagger}$	$\Delta E_4^{\ddagger}$ + ZPE	ν
BHandHLYP/6-311G**	12.5	18.4	122.1	112.2	366*i*	27.3	32.6	194.9	185.1	439*i*
BHandHLYP/cc-pVDZ	11.3	17.0	126.7	116.9	357*i*	25.2	30.3	196.7	186.3	428*i*
BHandHLYP/aug-cc-pVDZ	12.8	18.3	126.4	116.3	341*i*	29.8	34.8	200.0	189.7	422*i*
BHandHLYP/cc-pVTZ	15.8	21.6	119.7	109.8	369*i*	31.9	37.1	197.6	188.4	443*i*
QCISD/cc-pVDZ//BHandHLYP/cc-pVTZ	18.1	—	121.9	—	—	31.8	—	177.5	—	—
CCSD(T)/cc-pVDZ//BHandHLYP/cc-pVTZ	13.8	—	118.0	—	—	26.1	—	173.3	—	—
ROMP2/6-311G**//BHandHLYP/cc-pVTZ	8.4	—	112.8	—	—	26.0	—	189.7	—	—
G2//MP2(full)/6-31G*	16.2	—	100.2	—	—	38.3	—	183.0	—	—
G3(MP2)-RAD//BHandHLYP/cc-pVTZ	14.0	—	98.3	—	—	27.6	—	174.8	—	—

[a] Energies in kJ mol^{-1}. [b] Frequencies in cm^{-1}.

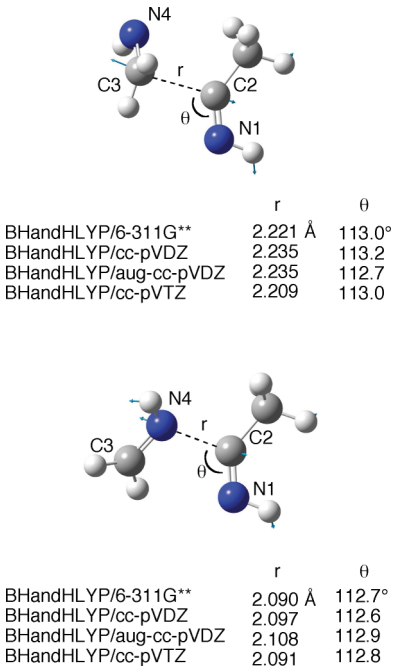

Fig. 1 Optimized structure of transition states **3** (upper) and **4** (lower) for the radical addition of methylimidoyl radical to the carbon and nitrogen ends of methanimine.

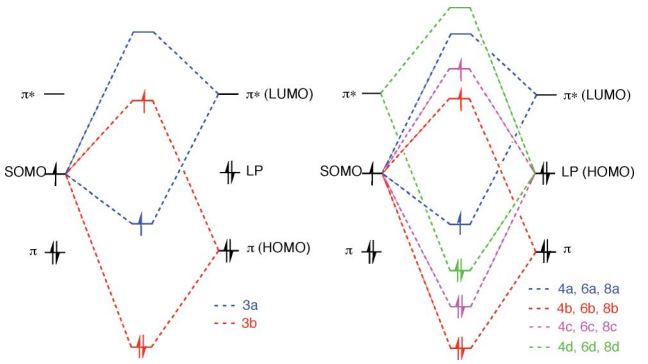

Fig. 2 Energy profile diagram for NBO analysis of orbital interactions for the homolytic addition of methylimidoyl radical to methanimine in transition states **3** (left) and **4**, **6**, **8** (right).

calculated using the G3(MP2)-RAD//BHandHLYP/cc-pVTZ method,[20] indicating that the BHandHLYP/6-311G** calculations perform as well as higher correlation techniques with larger basis sets.[23]

The data in Table 1 shows that the imidoyl radical has a significant preference for addition to the carbon end of the C=N bond this is in direct contrast with the acetyl radical, which is predicted to be unselective in its reaction with methanimine.[5]

Natural Bond Orbital (NBO) analysis at the BHandHLYP/6-311G** level of theory was carried out for both transition states. In the case of addition to the carbon end of the imine, NBO analysis reveals SOMO → π^*_{imine} and π_{imine} → SOMO interactions (Fig. 2, left). The former interaction, calculated to be worth 138 kJ mol^{-1}, is evident in the α spin-set, with the latter interaction in the β spin-set calculated to contribute 110 kJ mol^{-1} (Fig. 2, **3a** and **3b**). The nitrogen lone pair (calculated to be the HOMO of the imine) does not contribute to the developing interaction when the imidoyl radical attacks the carbon end of the imine. With the SOMO → π^*_{imine} interaction slightly larger than the π^*_{imine} → SOMO interaction, we can conclude that in its reaction at the carbon end of the imine the imidoyl radical acts as a moderately nucleophilic radical. Visualization of the Kohn–Sham orbitals generated at the same level of theory depicts the overlap of the two reacting units in transition state **3** (Fig. 3, left).

NBO analysis for attack of methylimidoyl radical at the nitrogen end of the imine again reveals SOMO → π^*_{imine} and π_{imine} → SOMO interactions, in this case worth 111 and 89 kJ mol^{-1}, respectively (Fig. 2, **4a** and **4b**). Interestingly, the latter interaction is not detected in the analogous reaction involving the acetyl radical. In addition, unlike the attack at the carbon end of the imine, a significant interaction (115 kJ mol^{-1}) between the unpaired imidoyl radical (SOMO) and the lone pair on nitrogen (imine HOMO) is observed in the β spin-set (Fig. 2, **4c**). Consequently, these data suggest that the imidoyl radical is acting as an electrophilic radical in its reaction at the nitrogen end of the C=N bond, in the same manner as the acetyl radical has been found to act in previous studies. A third interaction involving the nitrogen lone pair and the π* orbital of the imidoyl group is small, but apparent in both the α and β spin sets, is worth 17 kJ mol^{-1} (Fig. 2, **4d**). Although the calculated third interaction is smaller than those of acetyl and methoxycarbonyl radicals,[24,25] this interaction is responsible for the unusual transition state motion vectors in transition state **4** (Fig. 1). Inspection of the Kohn–Sham orbitals associated with

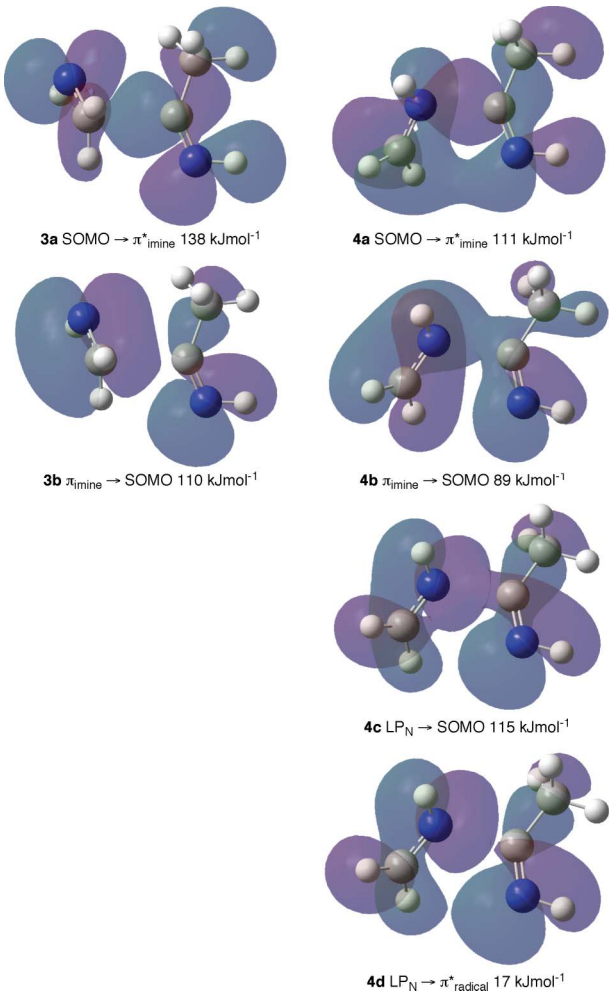

Fig. 3 BHandHLYP/6-311G** calculated Kohn–Sham orbitals involved in transition states **3** (left) and **4** (right).

this interaction reveal the secondary interactions complement the primary radical interactions and exist in order to maximize the energy gain from the available orbitals. It is interesting to note from the data in Table 1 that these reactions do not follow the Bell–Evans–Polanyi principle in that there appears to be no correlation between calculated energy barrier and exothermicity, which is perhaps not unexpected given the interesting orbital interactions involved during the addition at the nitrogen.

Reaction of the N-methylmethylimidoyl radical with methanimine

In order to further probe the influence of the methyl group on nitrogen in reactions involving imidoyl radicals, we next turned our attention to the reaction of N-methylmethylimidoyl radical ($\mathbf{1_{Me}}$) with methanimine (Scheme 4). Extensive searching of the relevant potential energy surfaces located transition state structures **5** and **6** for the addition to the carbon and nitrogen ends of methanimine, respectively. Optimized transition state structures of **5** and **6** are also displayed in Scheme 4 (at the BHandHLYP/cc-pVTZ level of theory). Geometrical data for the remaining levels of theory employed in this study are displayed in Fig. S1 of the ESI.‡ Not unsurprisingly, the transition state geometries are found to be very similar to those for the analogous reaction involving the

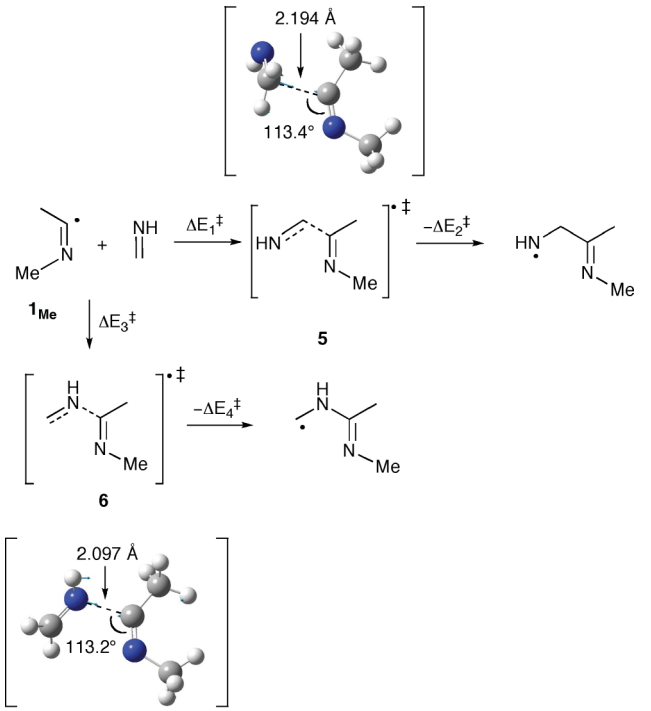

Scheme 4 BHandHLYP/cc-pVTZ optimized structure of transition states **5** (upper) and **6** (lower) for the radical addition of N-methyl-methylimidoyl radical ($\mathbf{1_{Me}}$) to the carbon and nitrogen ends of methanimine.

N-methylimidoyl radical. For example, at the BHandHLYP/cc-pVTZ level of theory, transition state separations for **5** and **6** are predicted to be 2.194 Å and 2.097 Å, respectively, as compared with the parent system whose transition state separations are 2.209 Å and 2.091 Å for **3** and **4**, respectively.

Selected activation energy data (Scheme 4, $\Delta E_1^{\ddagger} - \Delta E_4^{\ddagger}$) calculated are listed in Table 2, while a full listing at all levels of theory used in this study is available as Table S1 in the ESI.‡ Calculated energy barriers are also very similar to those for the methylimidoyl reactions, and again these reactions are predicted to be reasonably exothermic at all levels of theory. As shown in Table 2, the energy barriers for the forward reaction associated with transition states **5** and **6** are calculated to be 13.6 and 31.6 kJ mol^{-1}, respectively, at the BHandHLYP/6-311G** level of theory. Once again inclusion of ZPE correction serves to increase these barriers by about 5 kJ mol^{-1}, while improvement of basis set quality and levels of correlation has little effect on these barriers. For example at the G3(MP2)-RAD//BHandHLYP/cc-pVTZ level of theory, $\Delta E_1^{\ddagger}$ and $\Delta E_3^{\ddagger}$ are predicted to be 11.9 and 27.8 kJ mol^{-1}, respectively; indicating that the BHandHLYP/6-311G** calculations are performing comparably to the higher level calculations.

The data in Tables 2 and S1 (ESI‡) clearly show that addition of a methyl group on the nitrogen of the imidoyl radical has little effect on the calculated energy barriers for the reactions. As was observed for the methylimidoyl radical, the N-methylmethylimidoyl radical also shows significant preference for addition to the carbon end of the C=N bond.

Natural Bond Orbital (NBO) analysis at the BHandHLYP/6-311G** level of theory was carried out for both transition

Table 2 Calculated energy barriers[a] for the forward ($\Delta E_1^{\ddagger}$, $\Delta E_3^{\ddagger}$) and reverse ($\Delta E_2^{\ddagger}$, $\Delta E_4^{\ddagger}$) reactions of N-methylmethylimidoyl radical with methanimine and imaginary frequencies (ν)[b] of transition states **5** and **6** (Scheme 4)

	5					**6**				
Method	$\Delta E_1^{\ddagger}$	$\Delta E_1^{\ddagger}$ + ZPE	$\Delta E_2^{\ddagger}$	$\Delta E_2^{\ddagger}$ + ZPE	ν	$\Delta E_3^{\ddagger}$	$\Delta E_3^{\ddagger}$ + ZPE	$\Delta E_4^{\ddagger}$	$\Delta E_4^{\ddagger}$ + ZPE	ν
BHandHLYP/6-311G**	13.6	18.2	114.9	108.2	341*i*	31.6	35.0	187.1	180.3	410*i*
BHandHLYP/cc-pVTZ	16.6	21.3	112.0	105.4	341*i*	35.9	39.3	189.0	182.0	411*i*
CCSD(T)/cc-pVDZ//BHandHLYP/cc-pVTZ	13.7	—	111.2	—	—	28.8	—	167.7	—	—
G2//MP2(full)/6-31G*	13.9	—	96.9	—	—	41.3	—	179.9	—	—
G3(MP2)-RAD//BHandHLYP/cc-pVTZ	11.9	—	94.4	—	—	27.8	—	169.4	—	—

[a] Energies in kJ mol^{-1}. [b] Frequencies in cm^{-1}.

states and provided similar trends to those observed for the N-methylimidoyl radical. Kohn–Sham orbitals of transition states **5** and **6** were generated at the same level of theory and can be seen in Fig. S2 in the ESI.‡ In the case of addition to the carbon end of the imine, NBO analysis reveals SOMO → π^*_{imine} and π_{imine} → SOMO interactions are calculated to be 177 kJ mol^{-1} in the α spin-set, and 126 kJ mol^{-1} in the β spin-set. Since the SOMO → π^*_{imine} interaction is predicted to be stronger than the π^*_{imine} → SOMO interaction, and differences between these interactions is larger than those for the methylimidolyl radical, we can conclude that N-methylmethylimidoyl radical is more nucleophilic than the methylimidoyl radical for attack at the carbon end of the C═N bond of methanimine. Visualization of the Kohn–Sham orbitals in transition state **5** depicts similar overlap of the two reacting units as those observed for **3**.

NBO analysis for attack of N-methylmethylimidoyl radical at the nitrogen end of the imine reveals a similar trend to the parent system; the SOMO → π^*_{imine} and π_{imine} → SOMO interactions are worth 105 and 84 kJ mol^{-1} in the α and β spin-sets, respectively. A significant interaction (94 kJ mol^{-1}) between the unpaired N-methylmethylimidoyl radical (SOMO) and the lone pair of nitrogen (imine HOMO) is observed in the β spin-set. Consequently these data suggest that the N-methylimidoyl radical is acting as an electrophilic radical in its reaction at the nitrogen end of the C═N bond. A third interaction involving the nitrogen lone pair and the π* orbital of the N-methylimidoyl group is small, but apparent in both the α and β spin sets, and is worth 19 kJ mol^{-1}.

Reaction of the methanethioyl radical with methanimine

Extensive searching of the C_3H_6NS potential energy surface located transition state structures **7** and **8** for the addition of the methanethioyl radical (**2**) to the carbon and nitrogen ends of methanimine, respectively. The calculated energy barriers for the forward ($\Delta E_1^{\ddagger}$, $\Delta E_3^{\ddagger}$) and reverse ($\Delta E_2^{\ddagger}$, $\Delta E_4^{\ddagger}$) reactions (Scheme 5) and (imaginary) transition state vibrational frequencies are listed in Table 3. Optimized structures for **7** and **8** are displayed in Fig. 4, together with selected geometric features. Motion arrows associated with the transition state vector in each case are included and give insight into the attack trajectory of the methanethioyl radical during addition to the imine.§ Once again, transition state **7** shows similar rocking motion (ν = 344i cm^{-1}, BHandHLYP/6-311G**) to its acetyl counterpart.

The structures in Fig. 4 bear a striking resemblance to those calculated for the analogous reactions involving either the acetyl or imidoyl radicals. The transition state separations of **7** and **8** are

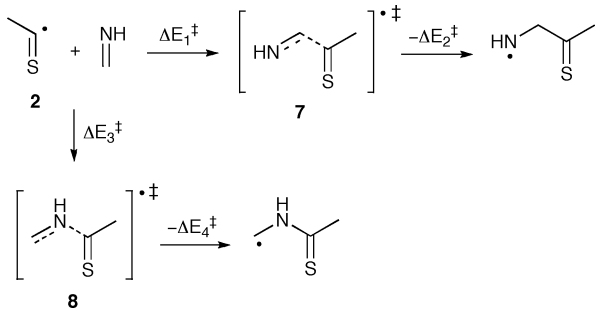

Scheme 5

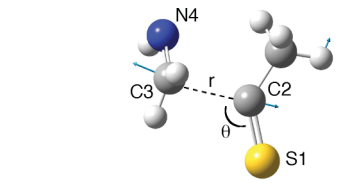

	r	θ
BHandHLYP/6-311G**	2.122 Å	117.5°
BHandHLYP/cc-pVDZ	2.134	118.0
BHandHLYP/aug-cc-pVDZ	2.134	117.2
BHandHLYP/cc-pVTZ	2.109	117.3

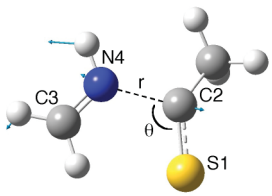

	r	θ
BHandHLYP/6-311G**	2.050 Å	110.0°
BHandHLYP/cc-pVDZ	2.050	109.8
BHandHLYP/aug-cc-pVDZ	2.068	109.5
BHandHLYP/cc-pVTZ	2.047	109.8

Fig. 4 Optimized structure of transition states **7** (upper) and **8** (lower) for the radical addition of methanethioyl radical to the carbon and nitrogen ends of methanimine.

predicted to lie within the range of 2.11–2.13 Å and 2.05–2.07 Å, respectively. The separations of **7** are around 0.05 Å smaller than those calculated for the analogous transition state involving the acetyl radical, while the separations of transition state **8** are some 0.1 Å larger than those involving the acetyl radical.

Table 3 Calculated energy barriers[a] for the forward ($\Delta E_1^{\ddagger}$, $\Delta E_3^{\ddagger}$) and reverse ($\Delta E_2^{\ddagger}$, $\Delta E_4^{\ddagger}$) reactions of methanethioyl radical with methanimine and imaginary frequencies (ν)[b] of transition states **7** and **8** (Scheme 5)

	7					**8**				
Method	$\Delta E_1^{\ddagger}$	$\Delta E_1^{\ddagger}$ + ZPE	$\Delta E_2^{\ddagger}$	$\Delta E_2^{\ddagger}$ + ZPE	ν	$\Delta E_3^{\ddagger}$	$\Delta E_3^{\ddagger}$ + ZPE	$\Delta E_4^{\ddagger}$	$\Delta E_4^{\ddagger}$ + ZPE	ν
BHandHLYP/6-311G**	24.8	29.9	98.9	93.2	498*i*	13.6	21.2	181.4	175.3	344*i*
BHandHLYP/cc-pVDZ	25.2	30.3	102.2	96.7	484*i*	11.2	18.9	182.1	176.2	337*i*
BHandHLYP/aug-cc-pVDZ	26.6	31.5	102.0	95.9	468*i*	18.7	26.2	184.6	178.0	338*i*
BHandHLYP/cc-pVTZ	31.1	36.1	95.9	90.2	504*i*	21.4	29.0	182.6	176.3	355*i*
QCISD/cc-pVDZ//BHandHLYP/cc-pVTZ	30.7	—	94.8	—	—	19.6	—	160.0	—	—
CCSD(T)/cc-pVDZ//BHandHLYP/cc-pVTZ	25.1	—	89.6	—	—	13.4	—	156.6	—	—
ROMP2/6-311G**//BHandHLYP/cc-pVTZ	8.9	—	73.7	—	—	15.1	—	166.9	—	—
G2//MP2(full)/6-31G*	26.2	—	79.6	—	—	15.7	—	160.0	—	—
G3(MP2)-RAD//BHandHLYP/cc-pVTZ	22.4	—	70.5	—	—	21.2	—	159.0	—	—

[a] Energies in kJ mol^{-1}. [b] Frequencies in cm^{-1}.

Inspection of Table 3 reveals that these reactions are predicted to be exothermic at all levels of theory employed in this study with calculated energy barriers ($\Delta E_2^{\ddagger}$ and $\Delta E_4^{\ddagger}$) for the reverse reactions (Scheme 5) consistently larger than those ($\Delta E_1^{\ddagger}$ and $\Delta E_3^{\ddagger}$) for the forward process. As shown in Table 3, the energy barriers for the forward reaction associated with transition states **7** and **8** are calculated to be 24.8 and 13.6 kJ mol^{-1}, respectively, at the BHandHLYP/6-311G** level of theory. Inclusion of ZPE correction and improvement of basis set quality increase the barriers by approximately 5 kJ mol^{-1} in each case. Most of the higher level calculations employed in this study, for example the CCSD(T) and G2 methods, afford similar barriers to those calculated at the BHandHLYP/6-311G** level of theory, however the QCISD calculation predicts barriers that are 5 kJ mol^{-1} higher in energy than the other levels of theory displayed in Table 3. The data in Table 3 shows that the methanethioyl radical preferentially adds to the nitrogen end of the C=N bond, with energy barriers ($\Delta E_3^{\ddagger}$) for addition to the nitrogen end of the imine calculated to be smaller (around 10 kJ mol^{-1}) than those ($\Delta E_1^{\ddagger}$) at the carbon end of the imine at all levels of theory (except the ROMP2 method). It is interesting to note that the thioyl radical favours addition to the nitrogen end of the C=N bond, exhibiting the opposite selectivity to the imidoyl radical ($\mathbf{1_H}$).

Natural Bond Orbital (NBO) analysis at the BHandHLYP/6-311G** level of theory was carried out for both transition states and provided some interesting trends. In the case of addition to the carbon end of the imine, NBO analysis reveals SOMO → π^*_{imine} and π_{imine} → SOMO interactions are calculated to be 200 kJ mol^{-1} (α spin-set) and 225 kJ mol^{-1} (β spin-set), respectively. Since the SOMO → π^*_{imine} interaction is predicted to be almost the same as the π^*_{imine} → SOMO interaction, we can conclude that the methanethioyl radical has an ambiphilic character for attack at the carbon end of the C=N bond of methanimine. Visualization of the Kohn–Sham orbitals in transition state **7** generated at the same level of theory depicts similar overlap of the two reacting units as those in **3** (Fig. 4, left).

Interestingly, NBO analysis for attack of the methanethioyl radical at the nitrogen end of the imine reveals that SOMO → π^*_{imine} and π_{imine} → SOMO interactions are very weak: worth 10 and 6 kJ mol^{-1} in the α and β spin-sets, respectively (Fig. 5, **8a** and **8b**). Instead, a large interaction (208 kJ mol^{-1}) between the unpaired methanethioyl radical (SOMO) and the lone pair of nitrogen (imine HOMO) is observed in the β spin-set (Fig. 5, **8c**).

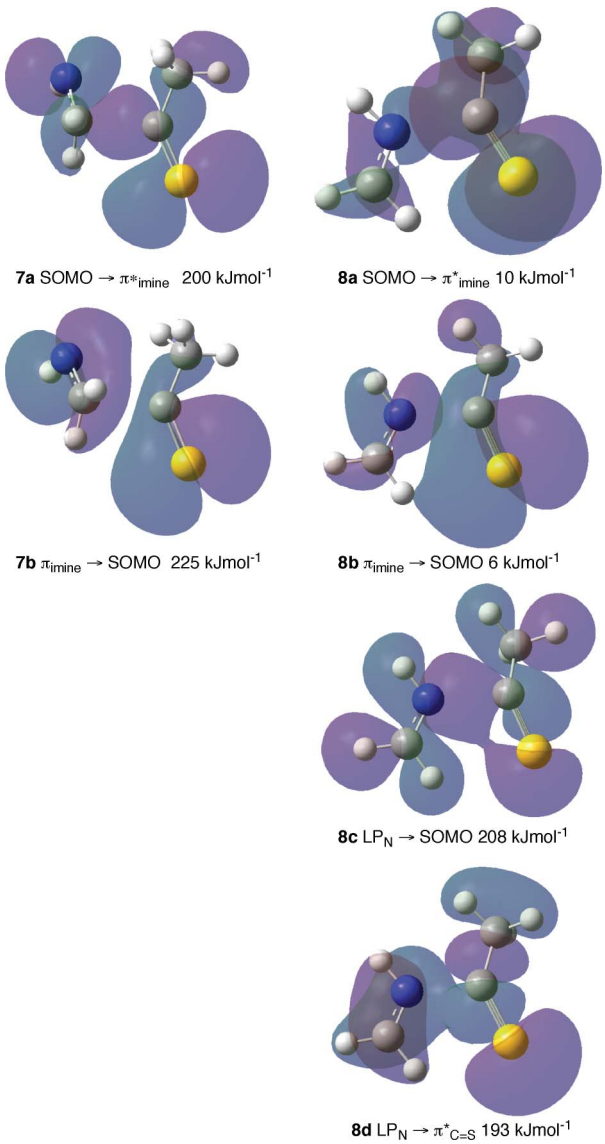

Fig. 5 BHandHLYP/6-311G** calculated Kohn–Sham orbitals involved in transition states **7** (left) and **8** (right).

Consequently, these data suggest that the methanethioyl radical is acting as an electrophilic radical in its reaction at the nitrogen end

of the C═N bond. A third interaction involving the nitrogen lone pair and the π* orbital of the thioyl radical is clearly apparent in both the α and β spin sets, and is worth 193 kJ mol^{-1} (Fig. 2, **8d**). The NBO analyses indicate that the methanethioyl radical reacts predominantly as an electrophilic radical.

Conclusions

This computational study has shown that imidoyl, N-methylimidoyl and thioyl radicals add to the nitrogen end of C═N bond in methanimine through SOMO → π^*_{imine}, π_{imine} → SOMO, LP_N → SOMO and LP_N → $\pi^*_{radical}$ interactions between the radicals and the imine. These multiorbital interactions are responsible for the unusual motion vectors associated with the transition states involved in the reactions. Comparing NBO results obtained in this study with those of the acetyl radical[22] reveals that LP_N → $\pi^*_{radical}$ interaction is very small in the reactions involving imidoyl and N-methylimidoyl radicals, while the SOMO → π^*_{imine} interaction is minimal in the reaction involving the thioyl radical. Consequently, we can conclude that reactions involving imidoyl radicals have more "classical radical" character while radical processes involving thioyl radical show more "ionic" character as comparison with reactions involving acetyl radical.

We applied the G3(MP2)-RAD calculation to all systems studied here and conclude that for radical processes involving acetyl and related radicals this method performs as well as the G2 method or CCSD(T) single-point calculations with larger basis sets. Indeed, at the G3(MP2)-RAD//BHandHLYP/cc-pVTZ level of theory the calculated energy barriers for the addition reaction of the acetyl radical to methanimine at the carbon and nitrogen ends of the imine are predicted to be 21.1 and 25.8 kJ mol^{-1}, respectively. It is interesting to compare these values with those calculated using the CCSD(T)/cc-pVDZ//BHandHLYP/cc-pVTZ method which provides values of 22.5 and 26.7 kJ mol^{-1}, respectively, while the G2//MP2(full)/6-31G* provides 22.4 and 18.2 kJ mol^{-1}. Interestingly of all the higher level calculations we conducted, only the G2 method shows preference for addition of the acetyl radical at the nitrogen end of methanimine, the preference that has been observed experimentally.

Acknowledgements

This work would not have been possible without the generous support of the Australian Research Council through the Centers of Excellence Program. We also gratefully acknowledge the support of the Victorian Institute for Chemical Science High Performance Computing Facility and the Australian Partnership for Advanced Computing National Facility. We thank Dr Michelle L. Coote for fruitful discussions and advice.

Notes and references

1 Selenoester: (*a*) J. Pfenninger, C. Heuberger and W. Graf, *Helv. Chim. Acta*, 1980, **63**, 2328; (*b*) C. E. Schwartz and D. P. Curran, *J. Am. Chem. Soc.*, 1990, **112**, 9272; (*c*) M. P. Astley and G. Pattenden, *Synlett*, 1991, 335; (*d*) D. L. Bonger and R. J. Mathvink, *J. Org. Chem.*, 1992, **57**, 1429; (*e*) P. A. Evans and J. D. Roseman, *Tetrahedron Lett.*, 1995, **36**, 31; (*f*) P. A. Evans and J. D. Roseman, *J. Org. Chem.*, 1996, **61**, 2252; (*g*) P. A. Evans and J. D. Roseman, *Tetrahedron Lett.*, 1997, **38**, 5249; (*h*) S. M. Allin,,W. R. S. Barton, W. R. Bowman and T. McInally, *Tetrahedron Lett.*, 2001, **42**, 7887.

2 Telluroester: (*a*) C. Chen, D. Crich and A. Papadatos, *J. Am. Chem. Soc.*, 1992, **114**, 8313; (*b*) C. Chen and D. Crich, *Tetrahedron Lett.*, 1993, **34**, 1545; (*c*) D. Crich, C. Chen, J.-T. Hwang, H. Yuan, A. Papadatos and R. I. Walter, *J. Am. Chem. Soc.*, 1994, **116**, 8937.

3 (*a*) I. Ryu, K. Matsu, S. Minakata and M. Komatsu, *J. Am. Chem. Soc.*, 1998, **120**, 5838; (*b*) M. Tojino, N. Otsuka, T. Fukuyama, H. Matsubara and I. Ryu, *J. Am. Chem. Soc.*, 2006, **128**, 7712; (*c*) S. H. Kyne, C. Y. Lin, I. Ryu, M. L. Coote and C. H. Schiesser, *Chem. Commun.*, 2010, **46**, 6521.

4 (*a*) C. H. Schiesser, H. Matsubara, I. Ritsner and U. Wille, *Chem. Commun.*, 2006, 1067; (*b*) C. T. Falzon, I. Ryu and C. H. Schiesser, *Chem. Commun.*, 2002, 2338; (*c*) H. Matsubara, C. T. Falzon and C. H. Schiesser, *Org. Biomol. Chem.*, 2006, **4**, 1920.

5 S. H. Kyne, C. H. Schiesser and H. Matsubara, *J. Org. Chem.*, 2008, **73**, 427.

6 S. H. Kyne, C. H. Schiesser and H. Matsubara, *Org. Biomol. Chem.*, 2007, **5**, 3938.

7 For a review see: M. Minozzi, D. Nanni and P. Spagnolo, *Curr. Org. Chem.*, 2007, **11**, 1366.

8 For some recent work see: (*a*) W. R. Bowman, A. J. Fletcher, P. J. Lovell and J. M. Pedersen, *Synlett*, 2004, 1905; (*b*) L. Benati, R. Leardini, M. Minozzi, D. Nanni, P. Spagnolo and G. Zanardi, *J. Org. Chem.*, 2000, **65**, 8669; (*c*) R. Leardini, D. Nanni and G. Zanardi, *J. Org. Chem.*, 2000, **65**, 2763; (*d*) S. Fujiwara, T. Matsuya, H. Maeda, T. Shin-ike, N. Kambe and N. Sonoda, *J. Org. Chem.*, 2001, **66**, 2183; (*e*) W. Du and D. P. Curran, *Org. Lett.*, 2003, **5**, 1765; (*f*) K. Tsuchii, Y. Tsuboi, S. Kawaguchi, J. Takahashi, N. Sonoda, A. Nomoto and A. Ogawa,, *J. Org. Chem.*, 2007, **72**, 415.

9 J. M. Pedersen, W. R. Bowman, M. R. J. Elsegood, A. J. Fletcher and P. J. Lovell, *J. Org. Chem.*, 2005, **70**, 10615.

10 H. Tokuyama and T. Fukuyama, *Chem. Rec.*, 2002, **2**, 37.

11 W. R. Bowman, A. J. Fletcher, J. M. Pedersen, P. J. Lovell, M. R. J. Elsegood, E. H. López, V. McKee and G. B. S. Potts, *Tetrahedron*, 2007, **63**, 191.

12 See reference 7 and papers cited therein.

13 M. Guerra, *J. Phys. Chem.*, 1996, **100**, 19350.

14 For some recent work see: (*a*) H. J. P. de Lijser, N. A. Rangel, M. A. Tetalman and C.-K. Tsai, *J. Org. Chem.*, 2007, **72**, 4126; (*b*) D. Nanni, G. Calestani, R. Leardini and G. Zanardi, *Eur. J. Org. Chem.*, 2000, 707.

15 Y. Gareau, R. Zamboni, J. Y. Gauthier and M. A. Bernstein, *Synth. Commun.*, 1995, **25**, 259.

16 T. Morihovitis, C. H. Schiesser and M. A. Skidmore, *J. Chem. Soc., Perkin Trans. 2*, 1999, 2041.

17 A. Alberti, M. Benaglia, M. Guerra, M. Gulea, D. Macciantelli and S. Masson, *Org. Lett.*, 2008, **10**, 3327.

18 For theoretical studies on thioyl radicals see: (*a*) I. McKenzie, J.-C. Brodovitch, K. Ghandi and P. W. Percival, *Phys. B*, 2006, **374–375**, 299; (*b*) V. Nevalainen and P. Vainiotalo, *Org. Mass Spectrom.*, 1987, **22**, 610.

19 M. J. Frisch, G. W. Trucks, H. B. Schlegel, G. E. Scuseria, M. A. Robb, J. R. Cheeseman, J. A. Montgomery, Jr., T. Vreven, K. N. Kudin, J. C. Burant, J. M. Millam, S. S. Iyengar, J. Tomasi, V. Barone, B. Mennucci, M. Cossi, G. Scalmani, N. Rega, G. A. Petersson, H. Nakatsuji, M. Hada, M. Ehara, K. Toyota, R. Fukuda, J. Hasegawa, M. Ishida, T. Nakajima, Y. Honda, O. Kitao, H. Nakai, M. Klene, X. Li, J. E. Knox, H. P. Hratchian, J. B. Cross, V. Bakken, C. Adamo, J. Jaramillo, R. Gomperts, R. E. Stratmann, O. Yazyev, A. J. Austin, R. Cammi, C. Pomelli, J. Ochterski, P. Y. Ayala, K. Morokuma, G. A. Voth, P. Salvador, J. J. Dannenberg, V. G. Zakrzewski, S. Dapprich, A. D. Daniels, M. C. Strain, O. Farkas, D. K. Malick, A. D. Rabuck, K. Raghavachari, J. B. Foresman, J. V. Ortiz, Q. Cui, A. G. Baboul, S. Clifford, J. Cioslowski, B. B. Stefanov, G. Liu, A. Liashenko, P. Piskorz, I. Komaromi, R. L. Martin, D. J. Fox, T. Keith, M. A. Al-Laham, C. Y. Peng, A. Nanayakkara, M. Challacombe, P. M. W. Gill, B. G. Johnson, W. Chen, M. W. Wong, C. Gonzalez and J. A. Pople, *GAUSSIAN 03 (Revision E.01)*, Gaussian Inc., Wallingford, CT, 2004; M. J. Frisch *et al.*, *GAUSSIAN 09 (Revision B.01)*, Gaussian Inc., Wallingford, CT, 2010.

20 D. J. Henry, M. B. Sullivan and L. Radom, *J. Chem. Phys.*, 2003, **118**, 4849.

21 E. D. Glendening, J. K. Badenhoop, A. E. Reed, J. E. Carpenter, J. A. Bohmann, C. M. Morales and F. Weinhold, *NBO 5.0*, Theoretical Chemistry Institute, University of Wisconsin, Madison, 2001.

22 The NBO method is a population analysis technique employed in computational chemistry to calculate the energies of orbital interactions within a molecule, and thus describes Lewis-like molecular bonding based on electron density between atoms in that molecule.
23 As has been shown in this study, the BHandHLYP/6-311G** method slightly overestimates the energies associated with formation of the nitrogen-attacked products, with $\Delta E_4^{\ddagger}$ calculated at this level of theory to be larger (by approximately 20 kJ mol^{-1}) than those obtained by the higher level calculations.
24 NBO analysis of addition of acetyl radical to the nitrogen end of methanimine provides SOMO $\rightarrow \pi^*_{imine}$ and $LP_N \rightarrow \pi^*_{radical}$ interactions are worth 90 and 138 kJ mol^{-1}, respectively. See reference 5.
25 NBO analysis of addition of methoxycarbonyl radical to the nitrogen end of methanimine provides a $LP_N \rightarrow \pi^*_{radical}$ interaction worth 55 kJ mol^{-1}. See reference 6.

